Cytotherapy 000 (2025) 1–11

Contents lists available at ScienceDirect

Full-length article

CYTOTHERAPY

journal homepage: www.isct-cytotherapy.org

International Society ISCT Cell & Gene Therapy®

Immunotherapy

Detailed analysis of the effects of a NOT gate on activation and growth of T cells

Yuta Ando, Jingli A. Zhang, Ethan A. McLeod, Jon Torres, Dongwoo R. Lee, Julyun Oh, Sanam Shafaattalab, Kelly C. Radecki, Kathleen Cunningham, Aaron D. Flynn, Nicolas Pedroncelli, Mark L. Sandberg, Breanna DiAndreth, Alexandre Zampieri, Jason Wang, Talar Tokatlian, Lu Min Wong, Han Xu, Alexander Kamb*

A2 Biotherapeutics, Agoura Hills, CA, USA

*Correspondence: Alexander Kamb, Ph.D., A2 Biotherapeutics, 30301 Agoura Road, Agoura Hills, CA 91301, USA. *E-mail address:* akamb@a2biotherapeutics.com (A. Kamb).

A B S T R A C T

Background aims: Dual-receptor NOT gates provide a mechanism to target effector cells to antigens that are absent in specific tissues, a situation that occurs frequently in cancer. For example, loss of heterozygosity (LOH) is a genetic event that removes large segments of one or the other homologous chromosome. Roughly 20% of the genes in an average solid tumor undergo LOH by the time of clonal neoplastic expansion, such that these irreversible genetic lesions are present in every cell of the tumor. To exploit this opportunity for selective targeting and other situations that arise in disease, a version of a NOT gate called Tmod™ technology has been developed. The Tmod platform incorporates two receptors: an activator based on a CAR or TCR, and a blocker based on the LIR-1 inhibitory receptor.

Methods: MHC class-I-regulated constructs display robust modularity, functioning well with a variety of activators—both CARs and TCRs—and blocker antigens encoded by different HLA class I alleles. We explore the details of activation, proliferation and cytotoxicity of the Tmod technology, focusing on a HER2 construct, but generalizing the conclusions by experiments with other Tmod constructs.

Results: We show that Tmod cells exhibit potent, selective tumor-killing even when surrounded by class-I-expressing cells in 3-dimensional spheroids *in vitro* and in the mouse body. This behavior is largely ligand-dependent, though there are small ligand-independent effects which are mainly ascribed to mechanisms other than the ITIM sequences of the LIR-1 blocker.

Conclusions: These detailed studies demonstrate that most of Tmod regulation is ligand dependent. Expression levels of the CAR affect activation/proliferation in a LIR-1 NOT gate, but the ITIM signaling module plays only a minor role in ligand-independent activity.

Key Words: blocker, cell engineering, iCAR, ITIM, spheroid, T cell proliferation, Tmod.

Introduction

In part because of the rarity of targets that are truly tumor-specific, cancer drug discoverers are increasingly focused on target profiles rather than single genes to achieve therapeutic windows [1,2]. Drug combinations and multi-specific soluble agents are approaches where drugs or binding functions are paired to gain efficacy and avoid additive toxicity [3,4]. Another strategy involves synthetic lethality, where inhibition of 2 or more targets in normal cells is tolerated, but inhibition in the cancer cell is crippling because of tumor-specific dependencies [5]. A third approach utilizes cells that are engineered to integrate multiple signals—sometimes called logic-gated cell therapy [6].

NOT gates are an especially attractive option in the logic-gate space. They substantially extend the range of potential cancer targets to antigens that are absent in cancer cells, due to either genetic loss (typically loss of heterozygosity, LOH) [7] or epigenetic differences [8]. The highly polymorphic and ubiquitously expressed HLA class I locus provides a convenient source of targets for a versatile NOT gate. For example, >60,000 deaths per year in the USA occur among patients with clonal HLA LOH in their tumors. Because such patients can be readily identified via genetic testing, NOT gate cell therapies such as Tmod are in development to leverage the binary allelic difference between tumor and normal cells in subsets of these patients (Figure 1A) [9,10]. The concept is to first identify germline-heterozygous HLA-A*02 patients whose tumors have lost the HLA-A*02 allele by LOH. These patients can be treated by Tmod constructs that comprise: (1) an activator antigen directed at a tumor-associated antigen such as CEA, MSLN, or EGFR; and (2) an inhibitory receptor ("blocker") directed at HLA-A*02 to protect non-tumor cells that express the activator antigens. Several such constructs gated by HLA-A*02 have been shown to display selective killing in 2-dimensional co-cultures and *in vivo* using a variety of dual-flank xenograft models [7,11–14].

We focus here on some of the more detailed features of the Tmod system related to the therapeutic window: selective activation, cytotoxicity, and proliferation. We concentrate on constructs derived from the clinical HER2 antibody trastuzumab (4D5). A trastuzumab-based HER2 CAR has been tested in the clinic, where it was fatal in the one patient treated, presumably due to on-target, off-tumor

https://doi.org/10.1016/j.jcyt.2025.06.014

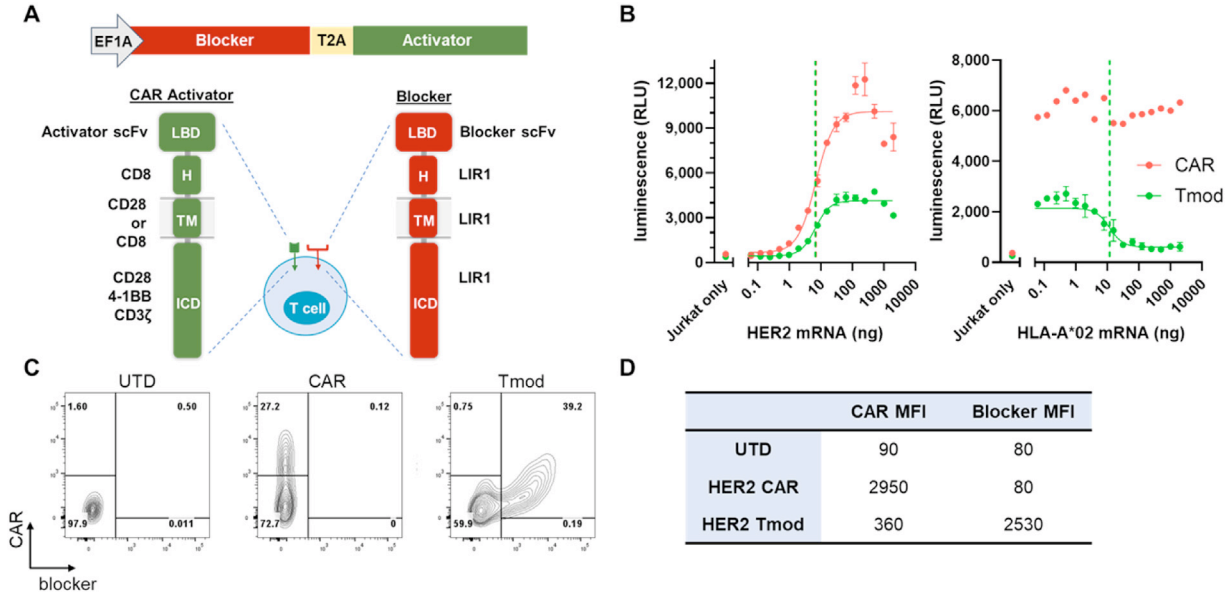

Fig. 1. HLA-A*02 NOT gate (HER2 Tmod). (A) Schematic of constructs used in Jurkat cells. HER2 scFvs were derived from clinical mAbs. HER2-targeting activator and HLA-A*02-targeting blocker receptors were co-expressed on a single lentiviral transcript using the EF1α promoter with a T2A translational pause/reinitiation site interposed between the coding sequences. (B) Ligand-dependent activation and inhibition in Jurkat cells using mRNA titration in HeLa target cells (see Methods). Dotted lines indicate interpolated EC50 and IC50 values. (C) Flow plots of CAR and blocker surface expression in both CAR-alone and Tmod constructs, as well as (D) the mean fluorescent intensity (MFI) of the signals.

toxicity [15]. This clinical result, as well as HER2's status as a tumor-associated antigen, makes HER2 CARs a compelling opportunity for resuscitation by incorporation into the Tmod logic gate. Because we seek general conclusions about the Tmod platform, we also study a variety of other Tmod constructs, some of which (CEA, MSLN, EGFR, HLA-E, and CD19) have been reported previously [7,11,12,14]. We show that although Tmod selectivity is largely ligand-dependent, Tmod cells have slightly reduced activation and proliferation compared to their cognate CARs. Crucially, despite this modest ligand-independent effect, robust potency and selectivity is maintained in complex environments; specifically, (1) 3-dimensional spheroid cocultures; and (2) a mouse model with a surrogate blocker that targets H-2D^b, a mouse class I paralog. In these biologically relevant settings, Tmod cells potently and selectively kill tumor cells. The tradeoff between potency and selectivity in the context of Tmod constructs and other therapeutics is discussed.

Results

Tmod constructs exhibit similar sensitivity versus CARs in Jurkat cell assays (but are selective)

While most of the activity of Tmod cells is demonstrably ligand-dependent [1,7], a set of experiments was undertaken to tease out more subtle quantitative effects on ligand-dependence in Jurkat cells using antigen-mRNA titration in HeLa target cells. The Tmod construct used for these experiments consisted of a single vector, with the activator encoded downstream of the blocker on the same transcript (Figure 1A). Importantly, the HER2 Tmod construct displayed ligand-dependent blocking, while the CAR was insensitive to expression of HLA-A*02 in HeLa cells (Figure 1B). The sensitivity (EC50) of both the HER2 CAR and Tmod construct, defined as the HER2 expression level in HeLa cells that generates half-maximal response in Jurkat cells that harbor an NFAT-regulated luciferase reporter, was estimated at ~7200 molecules/cell with the aid of calibration beads and standard curves (Figure S1). These sensitivities are in the range of previously measured values for CD19, MSLN, and EGFR constructs, and roughly 5x higher than for the CEA Tmod construct [11,12,14]. The maximum luciferase signal (E_{max}) in Jurkat cells was lower by ~2-4x for the HER2 Tmod construct compared to the HER2 CAR, consistent with a lower expression level (~8x) of the activator (Figure 1C,D) and with earlier studies linking E_{max} in Jurkat cells to activator expression level [16].

Tmod constructs exhibit slightly less acute potency versus CARs in primary T cell assays (but are selective)

Acute sensitivity to antigen of HER2 constructs was explored next in primary T cells. In these assays, an additional construct (HER2 Tmod(sh)) that contains a β_2-microglobulin (B2M) shRNA expressed from a separate promoter (Figure 2A), was included for comparison. The B2M shRNA module was developed previously to reduce the effects of cis-binding by endogenous HLA-A*02 molecules in HLA-A*02(+) donors [11]. mRNA titration using HER2(+ or -)HLA-A*02(+ or -) HeLa cells revealed clear antigen-dependent effects on activation and blocking (Figure 2B). These results were confirmed and extended using effector-to-target (E:T) titration assays in a second cell line, A375. For the E:T experiments, the constructs were tested in co-cultures with A375 cells of different genotypes: HER2(+)HLA-A*02 (-) tumor cells (target A) and HER2(+)HLA-A*02(+) "normal" cells (target AB) intended to mimic healthy cells in HLA-A*02 heterozygous patients, differing only by HLA-A*02 expression (Figure 2C,D). Averaged across 5 donors, the CAR was ~2x more potent than the HER2 Tmod and ~3.5x more potent than Tmod(sh) constructs. Importantly, Tmod and Tmod(sh) cells exhibited ~20x selectivity to distinguish tumor cells from "normal" cells, compared to their CAR counterparts (Figure 2D). IFN-γ measurements revealed that HER2 Tmod(sh) cells secreted ~3x less cytokine than CAR-Ts during the acute assay (Figure 2E).

To further explore acute behavior of the HER2 constructs, we measured short-term pseudo-markers of proliferation using polystyrene beads coated with different amounts of HER2 as the stimulus (Figure S2A,B). The beads activated cell division, based on the induction of the IL-2 receptor, CD25, in a ligand-dependent fashion (Figure S2C). HER2 CAR-Ts were the most sensitive, followed by Tmod and Tmod(sh). These results were confirmed by coculturing with A375 target cells and measuring Ki67 (Figure S2D). To quantify

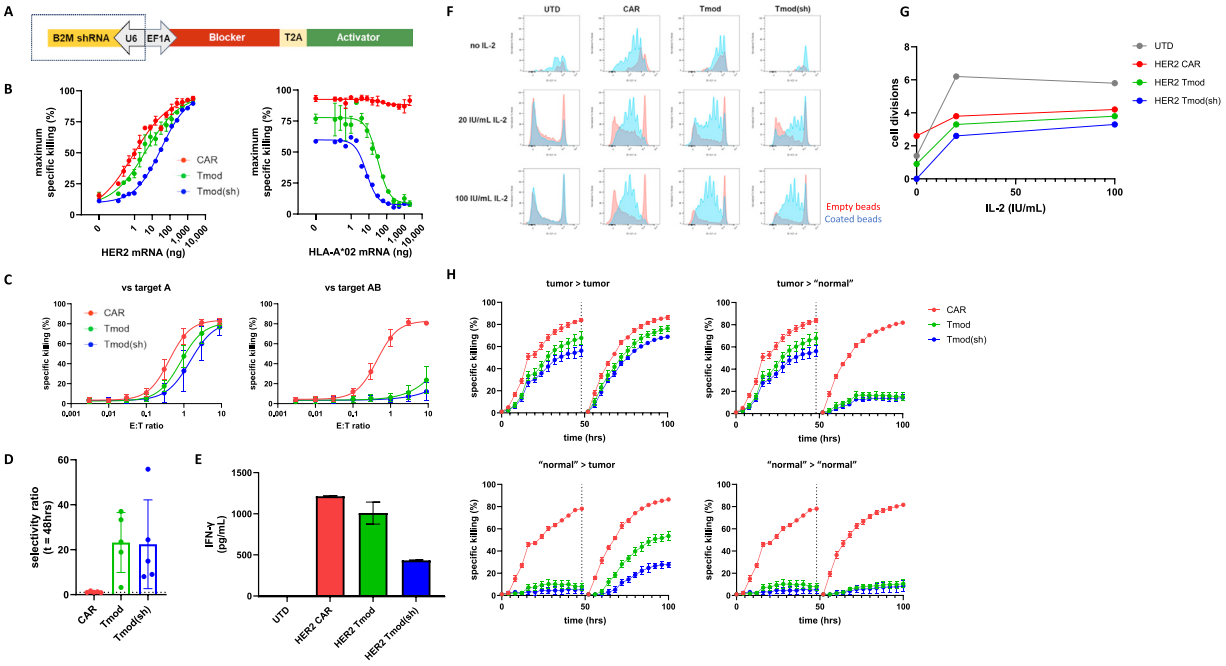

Fig. 2. Characterization of a HER2 | A*02 NOT gate (HER2 Tmod) in primary T cells. (A) Schematic of constructs used in primary T cells. Some constructs incorporate a B2M shRNA to reduce cis-binding by endogenous HLA-A*02 molecules in HLA-A*02(+) donor T cells. (B) mRNA titration using isotypes of HeLa target cells (see Methods). (C) E:T titration assays with HER2(+) A375 target cells of different genotypes, HER2(+)HLA-A*02(-) (target A) and HER2(+)HLA-A*02(+) (target AB). Cytotoxicity was measured at 48 hrs. The average and standard deviation are shown for 5 donors, 4 replicates each. (D) Bar graph of selectivity ratio calculated as the ratio of ET50 against target AB divided by ET50 against target A. Selectivity ratio is calculated with ET50 against target AB set to 27 if interpolated value > 27. (E) Cytokine secretion from acute killing assays was measured from the supernatant (see Methods). (F) Cell Trace Violet (CTV) fluorescence was assessed by flow cytometry at 6 days post stimulation by HER2-coated beads (see Methods). (G) Data from (F) plotted. (H) Killing was monitored over 2 days in cocultures with either tumor or "normal" A375 cells; then the T cells were transferred to fresh wells containing target cells and monitored for another 2 days (see Methods). Dotted lines segment each serial round.

cell proliferation, we tracked the dilution over time of a membrane-partitioning dye, Cell Trace Violet (CTV) at 3 different concentrations of IL-2 (0, 20, and 100 IU/mL). At 100 IU/mL IL-2, there was little difference among the constructs visible 6 days post-exposure to beads (Figure 2F,G). Without added IL-2, however, proliferation of the Tmod(sh) cells was considerably reduced compared to CAR-Ts; the HER2 Tmod cells were intermediate. These results indicated some difference among the constructs in acute antigen-stimulated activation/proliferation, with a general ranking of CAR > Tmod > Tmod(sh).

We next tested whether such differences were observed in a reversible-serial-killing assay in which effector T cells are transferred from one culture to fresh cultures of target cells in 2-day intervals. Though there was a small amount of apparent off-tumor killing, selectivity was largely preserved during serial transfer (Figure 2H). The low level of apparent background killing observed with "normal" cells may be a result of an allogeneic reaction and is observed in nearly all assays of this type, even when target cells without activator antigens are co-cultured with effector cells. This finding is consistent with data from other constructs, and with the high degree of selectivity displayed by mixed-target-cell cultures exposed to HER2 Tmod constructs (Figure S2E) [1,7]. Despite being activated (ON state) during co-culture with tumor cells, Tmod constructs rapidly returned to the OFF state after transfer to "normal" target cells. In contrast, all constructs (CAR, Tmod, Tmod(sh)) continued to kill after transfer from tumor-cell co-cultures to wells with fresh tumor cells. Accounting for a small lag to switch states, there was a modest, visible difference with regard to serial killing proficiency favoring the CAR over the Tmod construct.

Tmod cells proliferate slower without exogenous antigen than CAR- and untransduced T cells

In light of the small but reproducible differences among the HER2 constructs detected in acute assays, we compared the behavior of these constructs in longer-term assays. We reasoned that a small difference might be amplified over time. To estimate relative growth rates at longer intervals, we measured the percentage of receptor(+) cells in populations over time and normalized to the receptor(-) (i.e., untransduced) fraction. This subpopulation provided an internal control for proliferation.

For all constructs (CAR, Tmod, and Tmod(sh), the percentage of receptor(+) cells in these cultures grown in high concentrations of IL-2 (300 IU/mL) without target cells diminished slowly over time. Under conditions where the receptor(+) cells were enriched post transduction to nearly 100%, the "drift" of the population could be clearly determined. By 2 weeks post-enrichment, HER2 Tmod(sh) receptor(+) cells fell from 99% of the culture to 81% under the conditions tested (Figure 3A–C). HER2 CAR and HER2 Tmod cells drifted less, falling to 88–89% over the same interval. These results suggest that HER2 Tmod(sh) cells grow more slowly than HER2 CAR-Ts, a difference that becomes more apparent over time. Similar studies of CEA, MSLN, and EGFR constructs revealed the same pattern of growth difference: typically, CAR ≧ untransduced > Tmod > Tmod(sh) (Figure 3D). Thus, lower growth/survival of Tmod cells compared to CAR-only and untransduced cells is a general property of the Tmod platform, not necessarily related to the specific activator or target antigen. In serial antigen-stimulation assays where T cells were transferred every 2 days to wells with fresh target cells, the HER2 CAR was slightly more active than Tmod, a trend that became more apparent in the longer term (Figure S3A). CAR-Ts consistently have a small proliferative advantage compared to Tmod constructs.

Importantly, the basic proliferative and potency/selectivity properties of Tmod were confirmed in T cells derived from cancer patients using CEA Tmod(sh) (Figure S3B,C). Tmod cell expansion was similar to Tmod cells derived from a healthy donor, while potency and selectivity were maintained in an acutekilling setting.

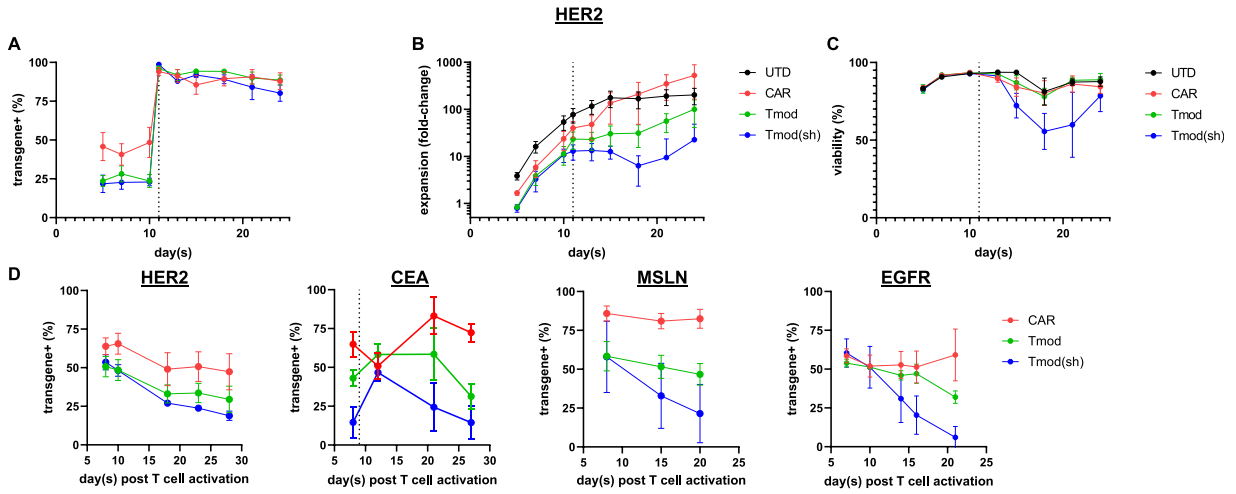

Fig. 3. Tmod cells proliferate at a slower rate vs. CAR-Ts and untransduced T cells. (A) Transgene(+) % of T cells transduced with lentivirus encoding HER2-targeting constructs was tracked for over 3 weeks. Cells were enriched on day 11 (dotted line). Data shown as average and SD of 6 donors. (B) The number of transduced T cells was tracked over time from total cell count and transgene(+) % from CAR and/or blocker receptor staining, then normalized by the initial cell count on day of thaw to calculate transduced T cell expansion in fold-changes . (C) T cell health during the same period was assessed via viability % reported from dead cell exclusion using propidium iodide (PI). Data shown as average and SD of 5 donors. Transgene(+) data from (D) HER2, CEA, MSLN, and EGFR Tmod cells display a similar trend in drift, suggesting that the Tmod platform exhibits modest anti-proliferative characteristics in the absence of antigen.

Differences in proliferation are multifactorial and not caused by specific signaling from the blocker ITIMs

Immune inhibitory receptors such as LIR-1 down-regulate T cell activation [17]. Most of their ligand-dependent inhibition requires the presence of ITIMs, short peptide motifs that contain conserved tyrosine residues within the intracellular domain of most inhibitory receptors. LIR-1, for instance, has 4 ITIMs, and robust blocker function requires that at least 2 are intact [7]. It is natural, therefore, to suppose that the slower growth of Tmod cells compared to CAR-Ts is related to overexpression of ITIM-containing receptors. Indeed, in Jurkat cells, expression of LIR-1 blockers reduces tonic signaling from CARs and this feature requires ITIMs [7].

We therefore tested blocker variants in which all the conserved ITIM tyrosines were mutated to phenylalanine, which abrogates interactions with inhibitory phosphatases [18]. For historical reasons, we used EGFR Tmod constructs for this comparison. Expression of the CARs in these constructs was similar to that observed with the HER2 Tmod construct: the CAR component expressed at ~2x higher levels in CAR-only cells vs. Tmod cells (Figure 4A,B). In long-term growth conditions with exogenous IL-2 (300 IU/ml) but without target cells, CAR-Ts eclipsed both Tmod and Tmod cells with mutated ITIMs (Tmod ITIM(-)) in total growth and in the proportion of receptor(+) cells (Figure 4C). Mutation of Tmod ITIMs did not impact drift; the proportion of receptor(+) cells declined similarly over the course of 18 days in culture. This result suggests that decreased proliferation observed with Tmod constructs is not caused by leaky or tonic inhibitory signaling by blocker ITIMs.

A second possibility is that the effect of Tmod on long-term proliferation is related to activator expression level in the dual-receptor Tmod context vs. CAR; that is, CAR expression is consistently higher in CAR-only designs because of the position of the CAR downstream of the blocker in the standard Tmod design, an orientation chosen for clinical safety reasons (Figure 1A). To test this possibility, we again used EGFR constructs and compared CAR to Tmod(sh) and Tmod(sh) super-transduced with additional CAR copies (Figure 4D; see Methods). This procedure created Tmod(sh) constructs (Tmod(sh)+CAR) with ~50% more CAR expression than Tmod(sh) (Figure 4E,F). When the receptor(+) populations of these T cells were tracked over time, Tmod(sh)+CAR cells drifted less than Tmod(sh) (Figure 4G,H), supporting the view that activator expression-level is partly responsible for the proliferation differences observed among the constructs. Furthermore, acute activation using beads titrated with different levels of EGFR antigen was also improved by overexpression of CAR in Tmod(sh) cells (Figure 4I,J). Therefore, we concluded that the absolute level of activator expression affects both antigen-dependent activation and antigen-independent proliferation of T cells. This latter effect of higher activator expression may be caused in part by increased tonic signaling from the CAR (see, for example, Figure 4I,J) [19].

Because we observed that Tmod(sh) cells are consistently slightly hypo-proliferative compared to non-shRNA-containing constructs, we investigated the possibility that higher B2M shRNA expression may be part of the explanation. To do this, T cell proliferation of different constructs was measured by CTV using antigen-coated beads as stimulus. By comparing Tmod cells to Tmod cells with B2M knocked out, we excluded the possibility that the effects on proliferation were caused by loss of B2M expression (Figure S4A). Next, we compared the effect of B2M shRNA expressed from 2 PolIII promoters, U6 and H1. U6 is known to be 5−10x stronger than H1 [20] and we have consistently observed larger reduction of B2M expression caused by U6-driven B2M shRNA compared to H1-driven shRNA [14]. In this experiment, the H1-B2M shRNA had little effect on proliferation, while the U6-B2M construct delayed proliferation, suggesting that higher shRNA burden may be part of the explanation for the differences in proliferation among the constructs (Figure S4B). Interestingly, proliferation differences were not observed when only the CAR was present, suggesting a potentially cumulative effect on growth caused by overexpression of both the shRNA and the blocker. Although this behavior might be unique to shRNA, we suspect it is related to general negative consequences of overexpression of genes in cells (see Discussion).

The HER2 Tmod construct is potent and selective in xenograft experiments

Having uncovered some differences *in vitro* with respect to activation/proliferation of HER2 Tmod cells compared to HER2 CAR-T cells and explored the mechanistic basis for these differences in related systems, we sought to examine further how these differences might manifest themselves in more complex physiological milieus. We focused initially on HER2 constructs, but extended the experiments to other Tmod constructs.

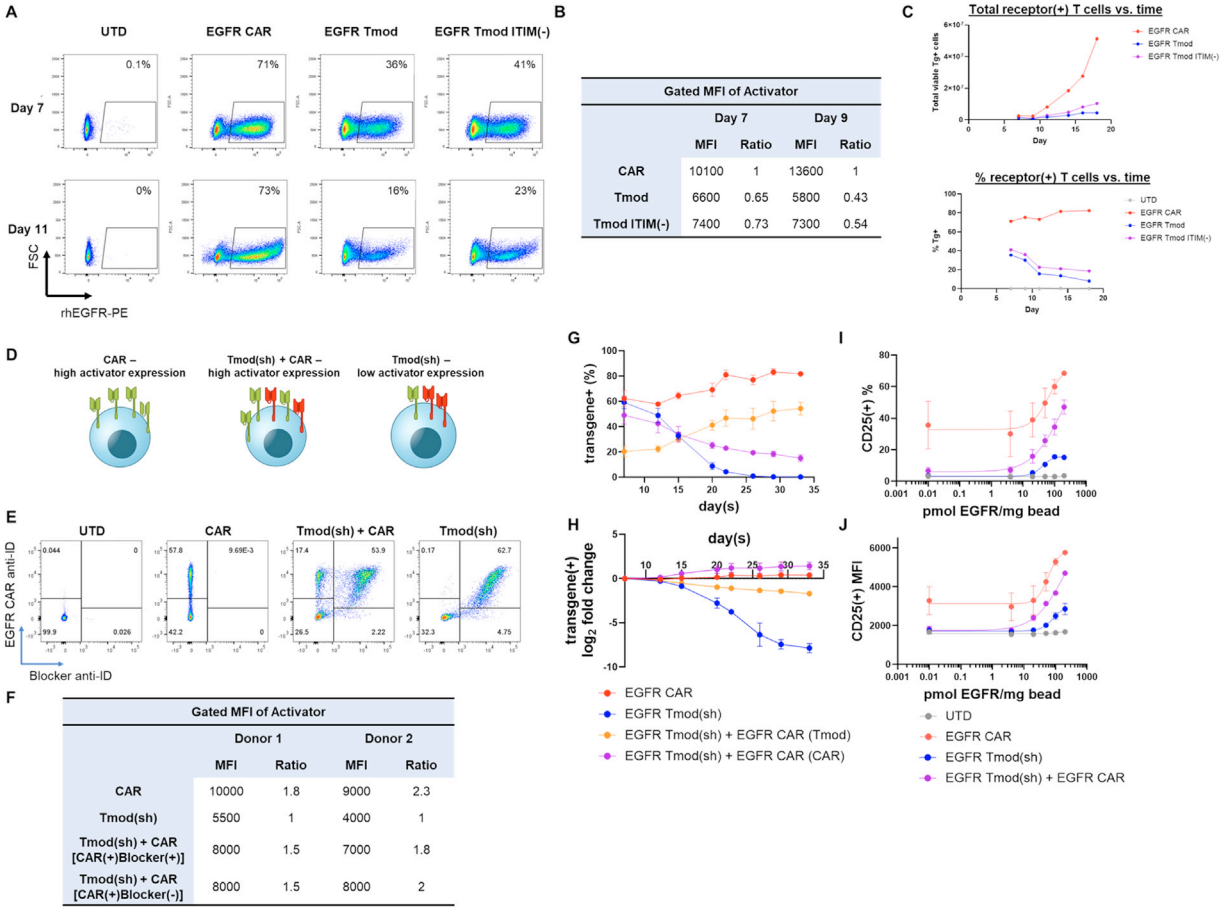

Fig. 4. Blocker ITIM mutations have miminal effect on antigen-independent growth (dirft) difference between receptor(+) and (-) populations, while activator expression level affects rate of drift and maximal activation. For these experiments, EGFR CAR and Tmod constructs were used. An EGFR Tmod variant with mutations in the ITIM conserved tyrosines (EGFR Tmod ITIM) was created. (A) Flow plot of activator expression and (B) quantification showing that activator expression is ~2x less in all EGFR Tmod constructs vs. CAR. (C) Viable cell count vs. time for EGFR constructs. See Methods for experimental details. (D) Cartoons of CAR = EGFR CAR-only; Tmod(sh) = EGFR Tmod(sh); Tmod(sh)+CAR = EGFR Tmod(sh) cells transduced with additional CAR vector (see Methods). (E) Flow cytometry data for constructs; staining with EGFR CAR anti-idiotype antibody and HLA-A*02 blocker anti-idiotype antibody. (F) Table with MFI quantification of expression levels in 2 donors on day 7. CAR(+)Blocker(+) refers to the double-positive population gated in the upper right quadrant of plots in (E). (G) Receptor(+) cells gated as in (E) were monitored for growth, normalized to the receptor(-) untransduced subpopulation, over time in 2 donors. (H) The fold-change from culture initiation is plotted. (I) CD25(+) T cells as a function of antigen concentration used to create EGFR bound to beads. (J) MFI of gated population from (A).

We began by conducting a two-flank xenograft study to compare the efficacy and selectivity of the Tmod constructs (Figure 5A). 2E7 cells of each construct, including an untransduced T cell control, were infused into the tail vein of mice harboring 2 types of established graft derived from the H508 cell line: (i) HER2(+)HLA-A*02(-) tumor graft; and (ii) HER2(+)HLA-A*02(+) "normal" graft. As expected from previous studies, HER2 Tmod constructs were both potent and selective, eliminating the tumor grafts but sparing the "normal" ones (Figure 5B,C). The HER2 CAR-Ts were also potent, but completely nonselective. Though detailed inspection of the graphs revealed a possible kinetic difference in the rate of tumor reduction, these differences were not statistically different. Measurement of human T cell levels in the mouse blood showed that Tmod(sh) cell levels were lower than CAR-T levels (Figure S5). However, the meaning of this difference was not clear because of the possibility that cells were not equilibrated between the blood and tumor.

We also attempted to test the constructs in xenografts with mixed populations of tumor and "normal" cells. However, for technical reasons, these experiments failed due to slight growth differences between the tumor and "normal" isogenic cell lines that were not apparent *in vitro*, but which manifested themselves *in vivo* (data not shown). The cell populations competed during the establishment of the mixed-cell graft *in vivo*, yielding uninterpretable results. We therefore explored other approaches to study the Tmod technology in complex milieus.

Tmod's potent, selective cytotoxicity is maintained in 3-dimensional spheroid co-cultures

To address the question of Tmod activity in complex settings in a different way, we created 3-dimensional spheroid cultures in which the isogenic tumor and "normal" lines were cultured long enough to form balls of cells prior to adding T cells (Figure 6A). This experimental setup allowed us to measure cytotoxicity under conditions where the Tmod and CAR T cells confront a complex milieu of 3-dimensional tumor and/or "normal" cells. The nature of the experimental setup precluded quantitative measurements of potency and selectivity. However, fluorescent reporters (GFP and RFP) expressed by the A375 isogenic lines used to assemble the spheroids enabled semi-qualitative analysis via imaging. The results were consistent with the previous studies that suggested a potency difference between HER2 Tmod and CAR; namely, the extent of killing in the spheroids of the tumor cells (HER2(+)HLA-A*02(-) A375) followed the rank order: CAR > Tmod > Tmod(sh). The selectivity of the Tmod constructs vs. CAR-Ts was dramatic, as observed in other assays. No killing of the "normal" cells (HER2(+)HLA-A*02(+) A375) was detected by Tmod and Tmod (sh) cells (Figure 6C; Figure S6B).

This experimental approach was repeated using a different Tmod construct (CEA Tmod) and isogenic cell line pair (H508). The CEA Tmod construct had previously been used in dual-flank H508 xenografts and displayed selective killing [11]. In this experiment, the

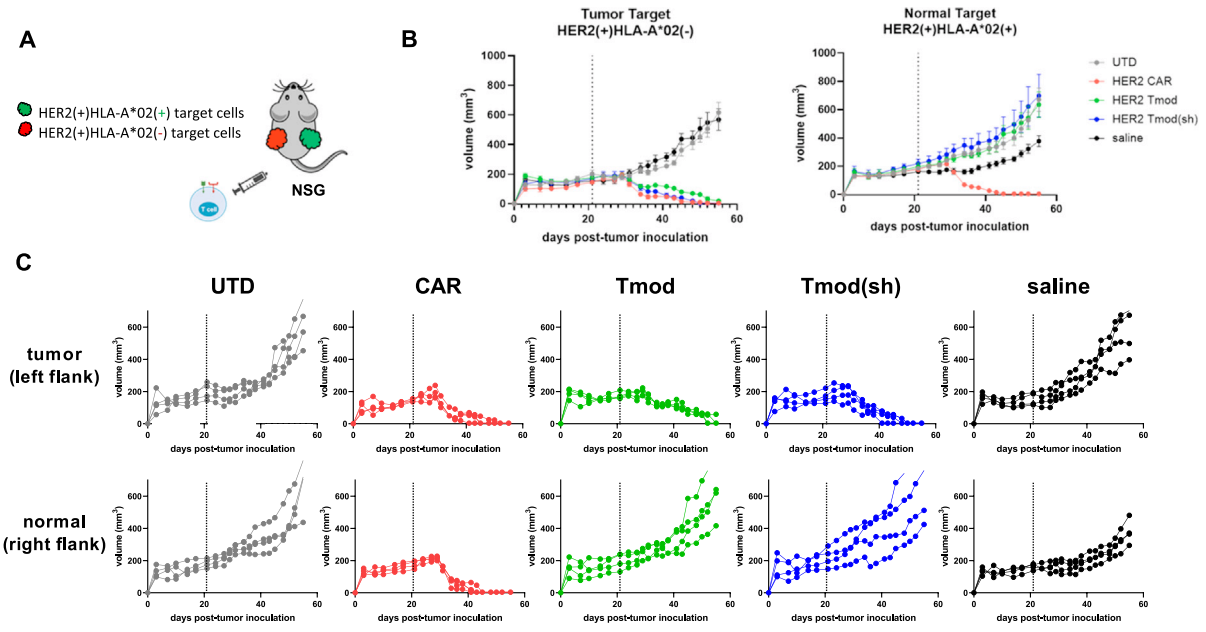

Fig. 5. HER2 Tmod and Tmod(sh) selectively kill H508 HER2(+)HLA-A*02(-) cells but not HER2(+)HLA-A*02(+) xenografts in NSG mice. (A) A dual-flank subcutaneous xenograft model where NSG mice were inoculated with HER2(+)HLA-A*02(-) tumor cells on the left flank and HER2(+)HLA-A*02(+) "normal" cells on the right flank were treated with 2E7 T cells from an HLA-A*02(-) donor transduced with single lentiviral vectors encoding HER2 CAR, HER2 Tmod, or HER2 Tmod(sh). (B) Tumor and "normal" xenograft volumes were derived from caliper measurements over time, showing selective killing of tumor targets by Tmod and Tmod(sh), but not CAR-T cells. Vertical lines indicate T cell injection. (C) Individual tumor volume measurements show no outliers.

spheroids were formed from mixtures of tumor and "normal" target cells. We also included normal fibroblasts from an HLA-A*02(+) donor at a 1:1 ratio with target cells to simulate stroma. These fibroblasts slightly slowed the kinetics of killing, possibly due to physical interference from the fibroblasts. However, the selectivity window was unaffected (Figure 6C; Figure S6B). This experimental setup also allowed us to compare Tmod selectivity in spheroid cultures with the gold standard of the adaptive cellular immune response, the T cell, using a clinical CEA TCR that recognizes a complex of HLA-A*02 and CEA peptide (residues 691-699) [21]. This CEA TCR was active in the clinic but severely toxic [22]. Qualitatively, the CEA Tmod constructs displayed a level of bystander killing of CEA(+)HLA-A*02(+) cells in the spheroid cocultures comparable to CEA TCR-T killing of bystander CEA(+)HLA-A*02(-)i cells. The results provide additional support for the robustness of the Tmod system; in particular, that it can integrate signals in a complex 3-dimensional setting and aim its cytotoxic arsenal as effectively as the cellular adaptive immune system, exemplified in this case by CEA TCR-Ts.

To summarize the findings in spheroid cultures, Tmod cells killed tumor cells with high selectivity compared to CAR-Ts, even in the

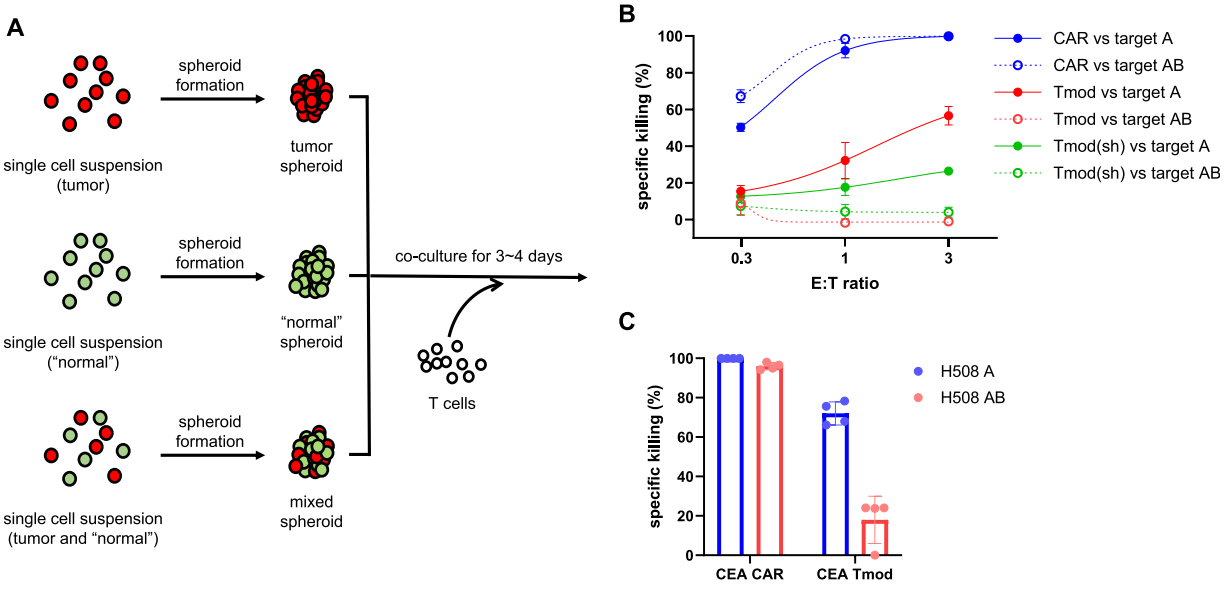

Fig. 6. (A) Schematic showing the workflow for 3D spheroid killing assay. (B) Quantification of fluorescence from images shown in Figure S4A. Target cells are A375 isogenic lines; A = HER2(+)HLA-A*02(-), labeled with an RFP constitutively-expressed reporter; AB = HER2(+)HLA-A*02(+), labeled with a constitutively-expressed GFP reporter. 4,000 T cells were seeded per spheroid and fluorescence was measured 96 hours later (see Methods). (C) Bar graph of data similar to (B) but using CEA Tmod constructs and H508 isogenic cell line pair: A = CEA(+)A*02(-) H508; AB = CEA(+)A*02(+) H508. Experiments conducted at E:T = 1:3.

presence of added normal fibroblasts. Some blunting of potency was evident compared to CAR-Ts, but it was not clear if this decrease in potency is intrinsic to the Tmod constructs or based on, for example, distraction by the HLA-A*02 blocker antigen that is expressed abundantly on the "normal" cells.

A surrogate Tmod construct regulated by H-2D^b mediates potent, selective killing of tumor cells in mice

To address the question of antigen distraction by normal tissues (i.e., interference by either biochemical binding to, or inhibition triggered by, the ubiquitously expressed blocker antigen in normal tissues), we developed a model for the function of Tmod cells in the mouse using a Tmod construct gated by the product of a mouse MHC class I paralog, H-2D^b ([14]; see Methods). We paired the H-2D^b blocker with a CD19 activator and used the CD19(+) Raji cell line engineered with HLA-A*02 and H-2D^b transgenes (Figure 7A). The Raji cells also expressed a luciferase reporter to permit quantification *in vivo* by bioluminescence.

Prior to testing *in vivo*, the Raji target cells were co-cultured with CD19 CAR, CD19 | HLA-A*02 Tmod, or CD19 | H-2D^b Tmod constructs to confirm expression and selective cytotoxicity *in vitro* of the Tmod constructs (Figure S7A,B). T cells were then infused into the tail veins of mice engrafted with the transgenic Raji cells and xenograft volume and bioluminescence was measured over time (Figure 7B,C). CD19 CAR-Ts killed both the parental Raji cells (CD19(+)) and the transgenic Raji cells (CD19(+)HLA-A*02(+)H-2D^b(+)). However, both Tmod constructs (CD19 | HLA-A*02 and CD19 | H-2D^b) killed only the parental Raji line. There was no difference in potency, suggesting that the ubiquitous expression of H-2D^b among mouse tissues did not distract the Tmod cells from killing their tumor targets. A slight difference in apparent selectivity was detected in this experiment, but given the large body of other *in vitro* and *in vivo* evidence, it was not considered meaningful. Blood human T cell levels were similar in animals treated with CAR and Tmod constructs, showing a slight rise and fall at early time points, consistent with clearing of the tumor, followed by an increase, likely the results of an allogeneic response visible clearly in the untransduced T cell cohort (Figure S7C). A similar *in vivo* experiment to measure Tmod potency/selectivity, where broad expression of the activator antigen in mouse tissues is shown to be overcome by the H-2D^b blocker, is discussed in a separate paper [14]. These results provide evidence that the Tmod system maintains potency and selectivity *in vivo* where there is a large preponderance of "normal" cells that express the MHC class I blocker antigen.

Discussion

Perhaps the most important property of a medicine is therapeutic window, a measure of efficacy compared to safety/tolerability. Because of the rapid mortality of many malignancies, oncology medicines have more leeway. Nonetheless, many cancer drugs are limited in efficacy due to toxicities that constrain their maximum dose. At present, discovery of better cancer medicines is hindered primarily by the shortage of new tumor-specific targets. For this reason, drug discoverers have begun to exploit the potential of antigen profiles using immune therapies.

The Tmod NOT gate has remarkable features and is able to demonstrate a selectivity window under a wide variety of experimental conditions; for example, when confronted by a vast excess of either activator or blocker antigen as described here and in previous publications. These Tmod properties, however, may come at a small but measurable cost of potency compared to CARs. The source of this ligand-independent effect on activation and proliferation is multifactorial. Based on data presented here, we can ascribe part of the effect to reduced activator surface expression levels in Tmod cells. This expression difference is caused by the construct design which encodes the 2 Tmod receptors (activator and blocker) on a single transcript, with the activator at the C-terminus. This design produces lower surface activator levels compared to the blocker. In addition to activator expression, the vector constructs likely place a burden on T cells caused by expression of multiple exogenous gene products, including the shRNA. Indeed, the differences on growth linked to shRNA driven by either the H1 or U6 promoter have been observed previously [23]. Conceptually, a simple way to offset the growth effects would be to increase expression of the activator as shown in Figure 4D. However, this approach has 2 problems. First, it risks overriding the blocker mechanism; and second, it may require

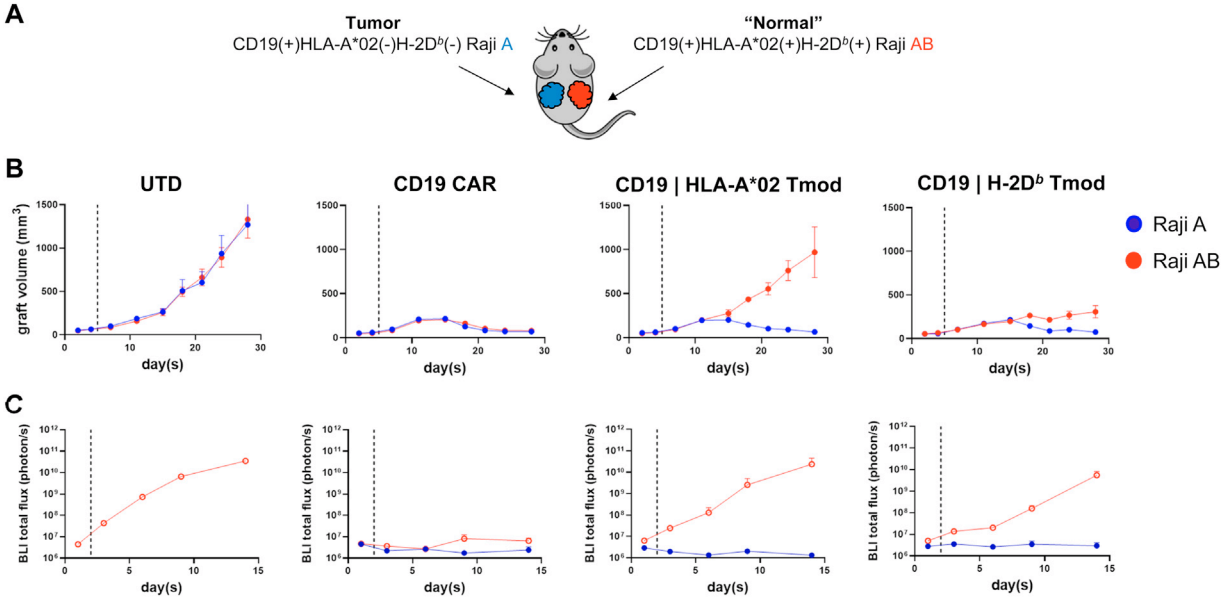

Fig 7. Potential distracting blocker antigen has minimal effect on efficacy. (A) Dual-flank Raji model setup of experiment with CD19 | H-2D^b and CD19 | HLA-A*02 Tmod constructs and controls. (B) Plots of tumor xenograft volume vs. time and (C) BLI vs. time for indicated constructs. Vertical lines indicate T cell injection. Dose = 1E7 T cells/mouse, % receptor(+) was ~90% for all cohorts.

engineering a different single-vector solution to the problem of activator-only-expressing T cells that occurs if 2 separate vectors are used for the blocker and activator, posing a potential safety risk.

Interestingly, the ITIMs do not appear to contribute much to antigen-independent growth differences between CAR and Tmod constructs. This observation appears to create a paradox: Limited tonic signaling benefits growth of T cells and Tmod quiets tonic signaling to a degree. If ITIMs reduce tonic signaling, how does the blocker cause a hypo-proliferative effect without intact ITIMs? Overexpression of proteins in cells places a burden on cell metabolism and growth [24–26] and membrane proteins are thought be more harmful at high levels because they can saturate the membrane-protein translocation apparatus [27]. Though a degree of tonic signaling from the activator may be beneficial in some circumstances and offset the negative effects of overexpression [19], it is likely that quantitative assays like many of those conducted here, will detect the cumulative small effects on growth caused by the burden of overexpression.

Importantly, the net effect of Tmod on therapeutic window, predicted from selectivity measured *in vitro* and *in vivo*, is strongly positive. A slight kinetic lag occurs when Tmod cells are transferred from "normal" to tumor target cells. This likely results from the assay conditions without exogenous IL-2 to maintain cell cycling. When the T cells are switched to tumor cells, they must reinitiate antigen-dependent activation. To deal with on-target, off-tumor problems of single antigens, some efforts have deliberately tuned down signaling and affinity of CARs to mitigate toxicity [28,29]. A similar strategy has been employed for bispecific T-cell engagers [30]. Such extreme measures may be required when the mechanism inherently lacks a therapeutic window. However, Tmod presents a rare opportunity to improve the potency of cancer therapies by eliminating biologic brakes and adding accelerators, because the starting point is a mechanism that confers high selectivity.

Though the LIR-1-based receptor has been generally adopted as the inhibitory module of NOT gates [13,31], other logic gates have been explored as possible therapeutics to widen the therapeutic window in oncology [1]. These logic gates recognize different, in some cases more complex, antigen profiles. Such logic gates include OR NOT, OR+NOT, and OR+OR NOT gates [1,31]. AND gates have also been devised but have proven more difficult to develop robustly [32]. A possible exception is an AND gate (LINK) that uses LAT and SLP76 signaling proteins, rather than ITAMs [33]. Finally, an AND that co-opts elements of Notch pathway signaling, perhaps better described as an IF THEN logic gate (SynNotch), has been advanced into the clinic [34,35].

The different mechanisms by which activation logic is enforced in immune effector cells have some tradeoffs. For example, with SynNotch the first antigen (A) triggers release of a transcription factor that translocates to the nucleus where it initiates expression of a CAR that allows T cell activation by a second antigen (B). This process results in delay between sensing of the first and second target antigens. In contrast, the LINK system is an AND gate with real-time signal-integration from the A and B antigens. Further studies should illuminate what tradeoffs are associated with the LINK approach; e.g., leakiness associated with constitutive overexpression of downstream signaling elements of the TCR pathway.

NOT gates like Tmod and its variants are also real-time signal integrators. Tmod has been studied in depth here and in a previous publication that demonstrates pharmacologic responses to target antigens across a range of antigen-level ratios [36]. However, though remarkably robust and modular, the sensitivity of the blocker may be a limiting factor because it must act in close proximity to the activator [37]. On the other hand, this proximity-sensing behavior is also a major strength. Unlike SynNotch, Tmod requires expression of the blocker antigen (B) on the same cell surface as the activator antigen (A). This feature, potentially shared by the LINK logic gate, allows discrimination of A(+)B(+) positive cells from A(+)B(-) cells in mixtures of target cells [7].

Conclusions

In aggregate, the data presented here shows that, although HER2 Tmod cells exhibit slightly lower acute potency than HER2 CAR-Ts, the large improvement in selectivity parameters *in vitro* and *in vivo* support the potential of dramatic improvement in the clinical on-target, off-tumor therapeutic window using the Tmod NOT gate. This situation encourages implementation of aggressive potency enhancements by adding booster modules, including but not limited to onboard cytokines [38].

Materials and Methods

Cell line generation and culturing

Unmodified HeLa, A375, NCI-H508 (H508), and Raji cells were purchased from ATCC. HeLa cells were cultured in MEM supplemented with 10% FBS and penicillin/streptomycin (P/S). A375 cells were cultured in DMEM supplemented with 10% FBS and P/S. H508 and Raji cells were cultured in RPMI supplemented with 15% FBS and P/S. To generate GFP(+), RFP(+), and luciferase(+) variants, cells were transduced with lentivirus encoding GFP, RFP, firefly-luciferase, or renilla-luciferase (Biosettia). To generate HLA-A*02(+) variants, cells were transduced with lentivirus encoding HLA-A*02 and FACS-sorted for HLA-A*02-positive cells using an HLA-A*02 antibody (clone BB7.2, Biolegend). H-2D^b(+) variants were generated in a similar manner using a lentivirus encoding H-2D^b and FACS-sorted for H-2D^b-positive cells using a H-2D^b antibody (clone KG95, eBioscience). To generate HER2(-) variants, CRISPR-Cas9 genetic modification was performed. Briefly, a mixture of 3 guide RNAs (gRNAs) targeting ERBB2 were purchased from Synthego, mixed with *Streptococcus pyogenes* HiFi Cas9 protein (IDT) at a 1:3 molar ratio to form ribonucleoprotein complexes, and transfected into cells using the Amaxa 4D nucleofection system (Lonza). Sequences for the gRNAs were: 1) CAUAGUUGUCCUCAAAGAGC, 2) AACAAUACCACCCCUGUCAC, and 3) CGCUCACAACCAAGUGAGGC. Jurkat cells with the NFAT-luciferase reporter system were purchased from BPS Bioscience and maintained in RPMI supplemented with 10% heat-inactivated FBS and P/S.

Molecular cloning

All CAR, Tmod, and Tmod(sh) constructs were cloned using Golden Gate assembly, where gene segments were combined and assembled downstream of a human EF1α, U6, or H1 promoter contained in a lentiviral expression plasmid. Activators were created by fusing scFv ligand binding domains (LBDs) to the CD8α hinge, CD8 or CD28 transmembrane domain, and CD28, 4-1BB, and CD3ζ intracellular domains. Blockers were generated by fusing scFv LBDs to the hinge, transmembrane domain, and intracellular domains of LIR-1. The HER2, EGFR, and CEA scFvs were derived from previous literature [11,14,39,40]. The H-2D^b scFv was identified by sequencing the 28-14-8S (HB-27) hybridoma (ATCC) using Genscript's hybridoma antibody sequencing service.

Quantification of activator and blocker sensitivity

HeLa target cells expressing activator and blocker antigen endogenously, recombinantly, or transiently via messenger RNA (mRNA) transfection were used for this determination. To control the degree of antigen expression on HeLa target cells with mRNA transfection, HER2 or HLA-A*02 mRNA were titrated into HER2 KO (HER2(-)HLA-A*02(-)) or wildtype (HER2(+)HLA-A*02(-)) HeLa cells, respectively, using the Amaxa 4D nucleofection system (Lonza). mRNA was

synthesized as previously described [11]. Antigen density was quantified using the QIFIKIT® (K007811-8, Agilent), used according to the manufacturer's protocol. Anti-HER2 (clone 24D2) and anti-HLA-A*02 (clone BB7.2) antibodies were used to confirm a titration of antigen expression in target cells.

Jurkat cells with the NFAT-luciferase reporter (JNL) were transfected with CAR or Tmod plasmid constructs using the Amaxa 4D nucleofection system. Transfected JNLs were co-cultured with target cells for 6 hours in the incubator, followed by measurement of luminescence on a plate reader (Spark® Multimode Microplate Reader) as a readout of Jurkat activation.

Primary T cell generation and characterization

Peripheral blood mononuclear cells (PBMCs) from healthy donors were purified from leukopaks purchased from HemaCare or Allcells. CD4(+) and CD8(+) T cells were enriched from PBMCs with Prodigy, according to manufacturer's protocols. These cells were then activated with TransAct (Miltenyi) and transduced with CAR- or Tmod- or Tmod(sh)-encoding lentivirus the next day at a multiplicity of infection (MOI) of 10-40. Transduced cells were cultured in G-Rex24 well plates (Wilson Wolf) with X-VIVO15 media (Lonza) supplemented with 1% human serum (GeminiBio) and P/S. Fresh IL-2 was added every 2-3 days at 300 IU/mL alongside media changes. For payload studies assessing various B2M modification strategies, T cells were either modified via CRISPR-Cas9 with a B2M gRNA or scramble gRNA 48-72 hours following lentiviral transduction. For *in vivo* studies, T cells were cultured in G-Rex6 well plates (Wilson Wolf).

Primary T cells were routinely counted and stained to check identity and track proliferation of transgene(+) cells. HER2 CAR was stained with either biotinylated Protein L (#29997, Thermo Fisher Scientific) or biotinylated HER2 recombinant protein (HE2-H82E2, ACROBiosystems) tetramerized with streptavidin conjugated to an appropriate fluorochrome. EGFR CAR was stained with biotinylated EGFR recombinant protein (EGR-H82E3, ACROBiosystems) tetramerized with streptavidin conjugated to an appropriate fluorochrome. The HLA-A*02 blocker was stained with either biotinylated peptide:HLA-A*02 probe tetramerized with streptavidin conjugated to an appropriate fluorochrome, generated as described previously [16] or an internally generated anti-HLA-A*02 antibody (clone 1G6.1).

Primary T cell in vitro *cytotoxicity assays*

T cells were prepared as described above. HER2 CAR, Tmod, or Tmod(sh) T cells were co-cultured with 2,000 HeLa or A375 target cells at defined E:T ratios in clear-bottom 384-well plates (Greiner). Briefly, target cells were seeded in quadruplicate wells of a 384-well imaging plate in 30 μL X-VIVO15 media supplemented with 1% human serum and P/S on day 1. For mixed culture assays, target cells (A and AB isotypes) were pre-mixed prior to seeding. For mRNA titration to assess CAR and blocker sensitivity in primary T cells, HER2(-) HLA-A*02(-) HeLa cells or HER2(+)HLA-A*02(-) HeLa cells were transiently transfected with a titration of HER2 mRNA or HLA-A*02 mRNA (2-fold, 16 points total), respectively, using the Amaxa 4D electroporation system (Lonza). Plates were incubated at 37°C, 5% CO_2 overnight to allow the cells to adhere. On day 2, T cells were added at appropriate E:T ratios in 30 μL X-VIVO15 media supplemented with 1% human serum and P/S. Plates were incubated at 37°C, 5% CO_2 and imaged every 4 hours for 48 hours using the ImageXpress Micro Confocal imager (IXM) with a 4x objective (Molecular Devices). Quantification of target cell area (i.e. GFP(+) or RFP(+) total area per image) was performed using MetaXpress analysis software, where surface area of GFP(+) or RFP(+) was quantified from background-subtracted fluorescence using an adaptive threshold. Plating variability was accounted for by normalizing to the area at time=0 for every well. Killing was then quantified as the difference in area between the test article vs corresponding untransduced T cell wells, normalized to the untransduced T cell well. For some acute killing assays, supernatant was collected and measured for IFN-γ concentration using the Cytometric Bead Array (CBA) human IFN-γ flex set (BD Biosciences).

For patients' primary T cells, samples were acquired from subjects with solid tumors who enrolled in clinical trials of Tmod therapies, which were approved by participating medical centers' Institutional Review Boards (IRBs). All subjects provided written informed consent in accordance with the Declaration of Helsinki and all ethical regulations were followed. These studies were registered at ClinicalTrials.gov (identifiers NCT04981119 and NCT06051695). For studies comparing patient-derived Tmod and healthy donor Tmod, CD56-depleted, CD4 and CD8 T cells (previously isolated using CliniMACS Prodigy and frozen) were thawed and cultured in X-VIVO 15 media (Lonza) supplemented with 300 IU/mL IL-2 (Bio-Techne), Physiologix (Nucleus Biologics) and GMP-grade TransAct (Miltenyi Biotec) following the manufacturer's guidelines in G-Rex 100M vessels (Wilson Wolf). 24 hours after stimulation, cells were transduced with lentivirus encoding CEA Tmod(sh) at a multiplicity of infection of 20. 24 hours after transduction, cells were topped off with additional supplemented X-VIVO 15 media and cultured for 5 days without disruption. On day 7 of culture, cells were harvested, characterized by flow cytometry and cryopreserved for future potency assessment (as described above).

Antigen-dependent stimulation assays

To characterize activation of primary T cells from activator antigen stimulation, T cells were cocultured with either antigen-coated beads or antigen-expressing A375 cells. To generate antigen-coated beads, streptavidin-coated M-280 Dynabeads (M-280-SA, Invitrogen) were washed with PBS with 0.1% BSA (FACS buffer) thrice and incubated with a forward titration of biotinylated recombinant HER2 protein and back-filled to saturation with a backward titration of an irrelevant, biotinylated mouse IgG1 kappa protein (DNP-BM190, ACROBiosystems). After 30 minutes, beads were washed with 1x PBS with 0.1% BSA and checked for coating efficiency with an anti-HER2 (clone 24D2) antibody. 1.5E5 microbeads were plated into U-bottom 96-well plates (Corning) in 100 μL X-VIVO15 media supplemented with 1% human serum and P/S. Next, 5E4 primary T cells were seeded into each well in 100 μL X-VIVO15 media supplemented with 1% human serum and P/S, making the final mixture a 200 μL volume with 3:1 bead-to-effector ratio. Positive control (T cells incubated with 1:100 TransAct) and negative controls (co-culture with un-coated Dynabeads, as well as T cells only) were included. After 24-48 hours of incubation, T cells were stained with a combination of Protein L and anti-CD25 (clone M-A251) antibody or anti-Ki67 (clone 11F6) after fixing and permeabilizing the membrane with the intracellular transcription factor staining buffer set (00-552300, Invitrogen), used according to manufacturer's protocol.

To examine proliferation of primary T cells from activator antigen stimulation, T cells were pre-stained with CellTrace Violet (CTV) (C34571, Invitrogen), according to the manufacturer's protocol, before coculturing with antigen-coated or un-coated Dynabeads as mentioned above. Culture conditions included 0, 20, or 100 IU/mL of IL-2. After 6 days in culture, cells were assessed on flow cytometry for CTV signal.

Blocker ITIM mutation assays

To assess the effect of the HLA-A*02 blocker on longer-term proliferation, EGFR CAR and Tmod constructs [14] were used. In order to

inactivate the blocker function, an EGFR Tmod variant was created by mutating all ITIM-conserved tyrosines to phenylalanine [7]. The EGFR CAR and Tmod variants were generated in primary T cells and maintained in culture as described above.

Controlling activator expression levels in primary T

To control CAR expression levels, EGFR CAR and Tmod(sh) constructs [14] were used. Primary T cells were transduced with either virus encoding for EGFR CAR only, EGFR Tmod(sh) only, or a mixture of the 2. T cells were maintained and periodically counted/stained as described above.

Understanding promoter strength on Tmod cell proliferation

CEA CAR and Tmod cells with different B2M modification strategies were prepared in primary T cells. B2M was modified via CRISPR-Cas9 gene modification or by having the B2M-targeting sequence downstream of either U6 or H1 promoters. As a control, un-modified CEA Tmod and CEA CAR with B2M knockdown via the U6 promoter were included. All T cells in this study were transfected with either gRNA targeting B2M or a scramble gRNA in order to eliminate the effect of transfection.

10 days post-TransAct activation, T cells were cocultured with either antigen-coated beads or un-coated beads for up to 7 days. To generate antigen-coated beads, streptavidin-coated M-280 Dynabeads (M-280-SA, Invitrogen) were washed with FACS buffer thrice and incubated with biotinylated recombinant CEACAM5 protein (ACROBiosystems). After 30 minutes, beads were washed with 1x PBS with 0.1% BSA and checked for coating efficiency with an anti-CEACAM5/CD66e (clone 487609) APC-conjugated antibody (FAB41281A, R&D Systems). 1.5E5 microbeads were plated into U-bottom 96-well plates (3799, Corning) in 100 μL X-VIVO15 media supplemented with 1% human serum and P/S. Next, 5E4 CTV-stained T cells were seeded into each well in another 100 μL X-VIVO15 media supplemented with 1% human serum and P/S, making the final mixture a 200 μL volume with 3:1 bead-to-effector ratio. At days 3, 5, and 7, cells were stained with an CD25 (M-A251) antibody and assessed by flow cytometry for CTV signal.

3D spheroid killing assay

In order to assess tumor killing by HER2-targeting T cells in a 3D setting, spheroids were generated. For HER2, A375 isogenic cells were used, including HER2(+)HLA-A*02(-)RFP(+) ffluc(+) target A, HER2(+)HLA-A*02(+)RFP(+) ffluc(+) target AB, and HER2(-)HLA-A*02(+)GFP(+) rluc(+) target B. 4,000 A375 cells were seeded in an ultra-low attachment 384-well plate (4516, Corning). For CEA, NCI-H508 isogenic cells were used, including CEA(+)HLA-A*02(-)RFP(+) ffluc(+) target A and CEA(+)HLA-A*02(+)GFP(+) rluc(+) target AB. 4,000 total H508 cells were seeded as described above. For mixed culture spheroids, 2,000 tumor and 2,000 "normal" H508 isotypes were mixed with or without 4,000 CCD-18Co fibroblast cells (ATCC, CRL-1459). After confirming spheroid formation, T cells were gently added at desired E:T ratios. Images of spheroids were obtained 96 hours after the addition of T cells by fluorescence microscopy (Keyence BZ X800) or confocal fluorescence microscopy (IXM). The percentage of specific killing at 96 hours was assessed by luciferase assay.

In vivo *studies*

In vivo experiments were conducted by Explora BioLabs or Charles River Accelerator and Development Lab (CRADL®) Thousand Oaks under Institutional Animal Care and Use Committee-approved protocols. The identities of target cells and T cells groups were blinded to the CROs. 5- to 6-week old female NOD SCID gamma (NSG; NOD.Cg-Prkdc^{scid}Il2rg^{1Wjl}/SzJ, JAX stock no. 005557) mice were purchased from the Jackson Laboratories. Animals were acclimated to the housing environment for at least 3 days before the initiation of the study.

In the dual-flank xenograft model testing the HER2-targeting constructs, animals were subcutaneously injected with HER2(+)HLA-A*02(-) "tumor" grafts on the left flank and HER2(+)HLA-A*02(+) "normal" grafts on the right flank. In the surrogate model, animals were subcutaneously injected with CD19(+)HLA-A*02(-)H-2D^{b}(-) Raji target A ("tumor") on the left flank and CD19(+)HLA-A*02(+)H-2D^{b}(+) Raji target AB ("normal") cells on the right flank. When xenografts reached an average of 100-160 mm^3, animals were randomized into groups and saline or T cells were administered intravenously through the tail vein. Xenograft volume measurements were performed by calipers 3 times per week for the duration of the study. Peripheral whole blood and serum were collected pre-T cell inoculation, and weekly from 6-days post T cell inoculation. Cells were stained post RBC lysis with anti-mouse CD45 (clone 30-F11), anti-human CD3 (clone UCHT1), anti-human CD4 (clone OKT4), anti-human CD8 (clone RPA-T8), and stained for CAR/blocker.

Statistical analysis

All *in vitro* data are shown as mean ± standard deviation, and *in vivo* data as mean ± standard error of the mean. *In vivo* tumor growth curves were compared using the Kruskal-Wallis statistical test. $P < 0.05$ was defined as statistically significant. For sensitivity and cytotoxicity assays, data points were fitted by a 4-parameter nonlinear regression analysis. EC50, IC50 and ET50 values were interpolated from fitted curves.

Declaration of Competing Interest

All authors are/were employees and shareholders of A2 Biotherapeutics, Inc. A.K. is a board member of A2 Biotherapeutics, Inc. Y.A., J.O., H.X., and A.K. are inventors of U.S. Patent # 11,730,764. B.D. and A.K. are inventors of U.S. Patent # 11,254,726.

Funding

This study was funded by A2 Biotherapeutics, Inc.

Author Contributions

Conceptualization, A.K., H.X., and Y.A.; Methodology, Y.A., J.A.Z., J.O., S.S., K.C.R., K.C., and A.D.F.; Investigation, Y.A., J.A.Z., E.A.M., J.T., D.R.L., J.O., S.S., K.C.R., K.C., A.D.G., N.P., M.L.S., B.D., A.Z., J.W., and T.T.; Writing – original draft, A.K.; Writing – review and editing, Y.A. and A.K.; Visualization, Y.A., J.A.Z, and A.K..; Supervision, Y.A., J.A.Z., M.L.S., L.M.W., H.X., A.K.; Funding acquisition, A.K. All authors have approved the final version of the manuscript.

Acknowledgments

We thank Aaron Martin for helpful discussions around the bead experiments involving costimulation, Chuck Li for assistance with high content imaging and automation, and Jun Wang (Explora BioLabs) and Celia Hanss (CRADL) for supervising *in vivo* experiments. We also thank colleagues from Technical Operations at A2 Biotherapeutics for manufacturing patient-derived Tmod cells.

Supplementary materials

Supplementary material associated with this article can be found in the online version at doi:10.1016/j.jcyt.2025.06.014.

Article History:

Received 11 February 2025
Accepted 29 June 2025
Available online xxx

References

[1] DiAndreth B, Hamburger AE, Xu H, Kamb A. The Tmod cellular logic gate as a solution for tumor-selective immunotherapy. Clin Immunol Orlando Fla 2022; 241:109030.
[2] Nix MA, Lareau CA, Verboon J, Kugler DG. Identifying optimal tumor-associated antigen combinations with single-cell genomics to enable multi-targeting therapies. Front Immunol 2024;15:1492782.
[3] Schmidt EV, Chisamore MJ, Chaney MF, Maradeo ME, Anderson J, Baltus GA, et al. Assessment of clinical activity of PD-1 checkpoint inhibitor combination therapies reported in clinical trials. JAMA Netw Open 2020;3:e1920833.
[4] Nolan-Stevaux O, Smith R. Logic-gated and contextual control of immunotherapy for solid tumors: contrasting multi-specific T cell engagers and CAR-T cell therapies. Front Immunol 2024;15:1490911.
[5] Ryan CJ, Devakumar LPS, Pettitt SJ, Lord CJ. Complex synthetic lethality in cancer. Nat Genet 2023;55:2039–48.
[6] Labanieh L, Mackall CL. CAR immune cells: design principles, resistance and the next generation. Nature 2023;614:635–48.
[7] Hamburger AE, DiAndreth B, Cui J, Daris ME, Munguia ML, Deshmukh K, et al. Engineered T cells directed at tumors with defined allelic loss. Mol Immunol 2020;128:298–310.
[8] Fedorov VD, Themeli M, Sadelain M. PD-1- and CTLA-4-based inhibitory chimeric antigen receptors (iCARs) divert off-target immunotherapy responses. Sci Transl Med 2013;5(215):215ra172.
[9] A2 Biotherapeutics Inc. *A phase 1/2 study to evaluate the safety and efficacy of A2B530, an autologous logic-gated Tmod™Chimeric Antigen Receptor T Cell (CAR T), in heterozygous HLA-A*02 adult subjects with recurrent unresectable, locally advanced, or metastatic solid tumors that express CEA and have lost HLA-A*02 expression*. https://clinicaltrials.gov/study/NCT05736731 (2024). Accessed June 23, 2025.
[10] A2 Biotherapeutics Inc. *A seamless phase 1/2 study to evaluate the safety and efficacy of A2B694, an autologous logic-gated Tmod™CAR T, in heterozygous HLA-A*02 adults with recurrent unresectable, locally advanced, or metastatic solid tumors that express MSLN and have lost HLA-A*02 expression*. https://clinicaltrials.gov/study/NCT06051695 (2024). Accessed June 23, 2025.
[11] Sandberg ML, Wang X, Martin AD, Nampe DP, Gabrelow GB, Li CZ, et al. A carcinoembryonic antigen-specific cell therapy selectively targets tumor cells with HLA loss of heterozygosity in vitro and in vivo. Sci Transl Med 2022;14:eabm0306.
[12] Tokatlian T, Asuelime GE, Mock J-Y, DiAndreth B, Sharma S, Toledo Warshaviak D, et al. Mesothelin-specific CAR-T cell therapy that incorporates an HLA-gated safety mechanism selectively kills tumor cells. J Immunother Cancer 2022;10:e003826.
[13] Bassan D, Weinberger L, Yi J, Kim T, Weist MR, Adams GB, et al. HER2 and HLA-A*02 dual CAR-T cells utilize LOH in a NOT logic gate to address on-target off-tumor toxicity. J Immunother Cancer 2023;11:e007426.
[14] Oh J, Kirsh C, Hsin J-P, Radecki KC, Zampieri A, Manry D, et al. NOT gated T cells that selectively target EGFR and other widely expressed tumor antigens. iScience 2024;27:109913.
[15] Morgan RA, Yang JC, Kitano M, Dudley ME, Laurencot CM, Rosenberg SA. Case report of a serious adverse event following the administration of T cells transduced with a chimeric antigen receptor recognizing ERBB2. Mol Ther J Am Soc Gene Ther 2010;18:843–51.
[16] Xu H, Hamburger AE, Mock J-Y, Wang X, Martin AD, Tokatlian T, et al. Structure-function relationships of chimeric antigen receptors in acute T cell responses to antigen. Mol Immunol 2020;126:56–64.
[17] De Louche CD, Roghanian A. Human inhibitory leukocyte Ig-like receptors: from immunotolerance to immunotherapy. JCI Insight 2022;7:e151553.
[18] Bellón T, Kitzig F, Sayós J, López-Botet M. Mutational analysis of immunoreceptor tyrosine-based inhibition motifs of the Ig-like transcript 2 (CD85j) leukocyte receptor1. J Immunol 2002;168:3351–9.
[19] Chen J, Qiu S, Li W, Wang K, Zhang Y, Yang H, et al. Tuning charge density of chimeric antigen receptor optimizes tonic signaling and CAR-T cell fitness. Cell Res 2023;33:341–54.
[20] An DS, Qin FX-F, Auyeung VC, Mao SH, Kung SKP, Baltimore D, et al. Optimization and functional effects of stable short hairpin RNA expression in primary human lymphocytes via lentiviral vectors. Mol Ther J Am Soc Gene Ther 2006;14:494–504.
[21] Parkhurst MR, Joo J, Riley JP, Yu Z, Li Y, Robbins PF, et al. Characterization of genetically modified T-cell receptors that recognize the CEA:691-699 peptide in the context of HLA-A2.1 on human colorectal cancer cells. Clin Cancer Res Off J Am Assoc Cancer Res 2009;15:169–80.
[22] Parkhurst MR, Yang JC, Langan RC, Dudley ME, Nathan D-AN, Feldman SA, et al. T cells targeting carcinoembryonic antigen can mediate regression of metastatic colorectal cancer but induce severe transient colitis. Mol Ther J Am Soc Gene Ther 2011;19:620–6.
[23] An DS, Qin FX-F, Auyeung VC, Mao SH, Kung SKP, Baltimore D, et al. Optimization and functional effects of stable short hairpin RNA expression in primary human lymphocytes via lentiviral vectors. Mol Ther J Am Soc Gene Ther 2006;14:494–504.
[24] Stoebel DM, Dean AM, Dykhuizen DE. The cost of expression of Escherichia coli lac operon proteins is in the process, not in the products. Genetics 2008;178: 1653–60.
[25] Bolognesi B, Lehner B. Reaching the limit. eLife 2018;7:e39804.
[26] Eguchi Y, Makanae K, Hasunuma T, Ishibashi Y, Kito K, Moriya H. Estimating the protein burden limit of yeast cells by measuring the expression limits of glycolytic proteins. eLife 2018;7:e34595.
[27] Wagner S, Baars L, Ytterberg AJ, Klussmeier A, Wagner CS, Nord O, et al. Consequences of membrane protein overexpression in Escherichia coli*. Mol Cell Proteomics 2007;6:1527–50.
[28] Schoutrop E, Poiret T, El-Serafi I, Zhao Y, He R, Moter A, et al. Tuned activation of MSLN-CAR T cells induces superior antitumor responses in ovarian cancer models. J Immunother Cancer 2023;11:e005691.
[29] Liu X, Jiang S, Fang C, Yang S, Olalere D, Pequignot EC, et al. Affinity-tuned ErbB2 or EGFR chimeric antigen receptor T cells exhibit an increased therapeutic index against tumors in mice. Cancer Res 2015;75:3596–607.
[30] Vafa O, Trinklein ND. Perspective: designing T-cell engagers with better therapeutic windows. Front Oncol 2020;10:446.
[31] Frankel NW, Deng H, Yucel G, Gainer M, Leemans N, Lam A, et al. Precision off-the-shelf natural killer cell therapies for oncology with logic-gated gene circuits. Cell Rep 2024;43(5):114145.
[32] Cho JH, Collins JJ, Wong WW. Universal chimeric antigen receptors for multiplexed and logical control of T cell responses. Cell 2018;173:1426–38.
[33] Tousley AM, Rotiroti MC, Labanieh L, Rysavy LW, Kim W-J, Lareau C, et al. Co-opting signalling molecules enables logic-gated control of CAR T cells. Nature 2023;615:507–16.
[34] Morsut L, Roybal KT, Xiong X, Gordley RM, Coyle SM, Thomson M, et al. Engineering customized cell sensing and response behaviors using synthetic notch receptors. Cell 2016;164:780–91.
[35] Okada, H. *Phase 1 study of autologous anti-EGFRvIII SynNotch receptor induced anti-EphA2/IL-13R Alpha2 CAR (E-SYNC) T cells in adult participants with EGFRvIII+ glioblastoma*. https://clinicaltrials.gov/study/NCT06186401 (2025). Accessed June 23, 2025.
[36] Manry D, Bolanos K, DiAndreth B, Mock J-Y, Kamb A. Robust in vitro pharmacology of tmod, a synthetic dual-signal integrator for cancer cell therapy. Front Immunol 2022;13:826747.
[37] Mock J-Y, Winters A, Riley TP, Bruno R, Naradikian MS, Sharma S, et al. HLA-A*02-gated safety switch for cancer therapy has exquisite specificity for its allelic target antigen. Mol Ther - Oncolytics 2022;27:157–66.
[38] Zhang JA, Imboden S, Lee D, Zampieri A, Shafaattalab S, Liang J, et al. Onboard, tethered IL-12 boosts potency of the Tmod NOT gate and preserves selectivity. J Immunother Cancer 2025;13:e010976.
[39] Zhao Y, Wang QJ, Yang S, Kochenderfer JN, Zheng Z, Zhong X, et al. A herceptin-based chimeric antigen receptor with modified signaling domains leads to enhanced survival of transduced T lymphocytes and antitumor activity. J Immunol Baltim Md 1950 2009;183:5563–74.
[40] Bryant, J. L. HERCEPTIN adjuvant therapy. US Patent US20060275305A1 (2006).